International Journal of Material Forming (2022) 15: 43
https://doi.org/10.1007/s12289-022-01694-4

DEVELOPMENTS IN MODELLING AND SIMULATION..JAPAN, SOUTH KOREA AND CHINA

Plastic flow localization resulting from yield surface vertices: crystal plasticity and corner theories of plasticity

Mitsutoshi Kuroda[1]

Received: 20 May 2021 / Accepted: 18 April 2022 / Published online: 27 April 2022

Abstract
This article describes the fundamentals and importance of the yield surface vertex effects in plastic flow localization predictions. The yield surface vertex effects are inherent in crystal plasticity based on Schmid law and have been elaborated in phenomenological corner plasticity theories. First, the theoretical importance, experimental evidence and modeling strategies of the yield surface vertices are presented. Next, plastic flow localization analyses using the yield surface vertex effects in previous studies are reviewed. Both full-field analyses by the finite element method and simplified analyses (i.e., Marciniak–Kuczynski-type of approach) are considered. It is also to be noted that conventional plasticity theories (including both phenomenological and crystal plasticity theories) do not involve any intrinsic material length-scale effects. This could lead to drawbacks in applications and plastic flow localization analyses, because these theories do not enable to predict shear bands with width of finite size. We conclude with the presentation and review of recent developments of gradient-enhanced vertex-type plasticity and crystal plasticity theories.

Keywords Yield surface vertex · Crystal plasticity · Corner theory of plasticity · Imperfection · Bifurcation · Strain gradient plasticity

Introduction

With material models involving classical smooth yield surfaces, there are difficulties in predicting plastic flow localization particularly in the form of shear bands in materials in bulk form or in predicting necking for biaxially stretched sheets. Plastic flow localization is possibly induced by (i) the yield surface vertex effect [1, 2], (ii) dilatational plastic flow accompanying macroscopic softening due to evolving damage (nucleation and growth of voids) [3, 4], (iii) thermal softening in adiabatic or high-speed deformation [5], and (iv) deviations from the normality rule for plastic flow arising, for example, in a material exhibiting a hydrostatic stress dependence [6]. Although each of these mechanisms have a significant destabilizing effect independently, combinations of these mechanisms play a dominant role in causing plastic flow localization, depending on the material, and for a given material, on the stress state. Generally, plastic flow localization suddenly appears from a nearly uniform straining state at a certain stage of overall deformation under isothermal conditions even with neither clear indication of damage evolution nor hydrostatic dependence of yielding. This is a consequence of the vertex effect inherently existing in crystalline materials, which makes possible the situation where two or more modes of strain rate exist under a fixed stress state. In this regard, the vertex effect is the most fundamental and important among the four factors described above in plastic flow localization problems. The crystal plasticity model [7] innately equips this effect [2, 8, 9]. To mimic the vertex effect, various phenomenological corner theories of plasticity have been proposed (e.g., [10–17]). The present article focuses on the fundamentals, modeling and applications of the vertex effect.

✉ Mitsutoshi Kuroda
kuroda@yz.yamagata-u.ac.jp

[1] Mechanical Engineering, Yamagata University, Jonan 4-3-16, Yonezawa, Yamagata 992-8510, Japan

Vertices on the yield surface

The question of the existence of corners (or vertices) on the yield surface had long been of particular interest in the field of the mechanics of inelastic materials. Whether or not a vertex forms on the yield surface is very important in cases where deviations from proportional loading occur, e.g., predictions of plastic instability, e.g., [10, 18]. The conventional normality flow rule does not account for sheet necking in biaxial tension at realistic stress and strain levels without the introduction of a large geometrical imperfection, while incorporating the corner concept results in a realistic sheet necking behavior that is in agreement with general experimental observations [10]. The standard normality flow rule never predicts shear band formation in a bulk material having a positive strain hardening modulus [19, 20], while the introduction of the corner concept naturally leads to predictions of shear band development [21]. A flow rule with corners predicts much lower buckling loads (in agreement with general experimental observations) than those computed using conventional theories with smooth yield loci [22] (see also discussion by Hutchinson [23]). In general, plastic flow localization suddenly appears from a uniform straining state at a certain stage of deformation. This means that two or more modes of the plastic strain rate may possibly appear for a fixed stress state. To establish this peculiar situation, the existence of a vertex at the loading point on the yield surface is conceptually necessary. In the case of rate-independent elastoplasticity, the sudden change in the plastic strain rate mode without any change in the stress state corresponds to *bifurcation*. When the material has a rate dependence, the vertex is considered not to be an actual sharp vertex, but to be a portion of the yield surface with a high curvature, the so-called *rounded vertex*.

The existence of corners is plainly explained for single crystals [8]. Figure 1(a) schematically shows corners on the yield surface of a single crystal. If the material deforms by a single slip, a *normality* flow occurs since a standard associated flow rule is assumed for a yield plane of a single slip system. Once a double- or multislip state is established, the stress point must be on a line of intersection between two yield planes or on a corner of the hyper-polyhedron consisting of the yield planes for the crystallographic slip systems. Thus, it is theoretically obvious that single crystals have corners on their yield surface. Asaro [8] pointed out that the corners on the yield surface can promote localized shearing even for slip hardening materials. When the material rate dependence is considered [24], all the slip systems are potentially active. In this case, the vertex is not sharp, but is a portion of the yield surface with a high curvature. From an engineering point of view, particular interest had been on whether or not corners exist in general polycrystalline metals. Hutchinson [2] illustrated yield surfaces of a face-centered cubic (FCC) polycrystal by self-consistent [1, 25] computations and showed that a corner develops at the stress point on a shear stress–normal stress cross section of the yield surface after tensile loading. However, most experimentally determined yield surfaces did not exhibit corners, but they were observed to be smooth or rounded. Hecker [26] surveyed 54 experimental studies on attempts to detect corners on the yield surface, and summarized that only five detected sharp corners, 16 observed rounded corners, and

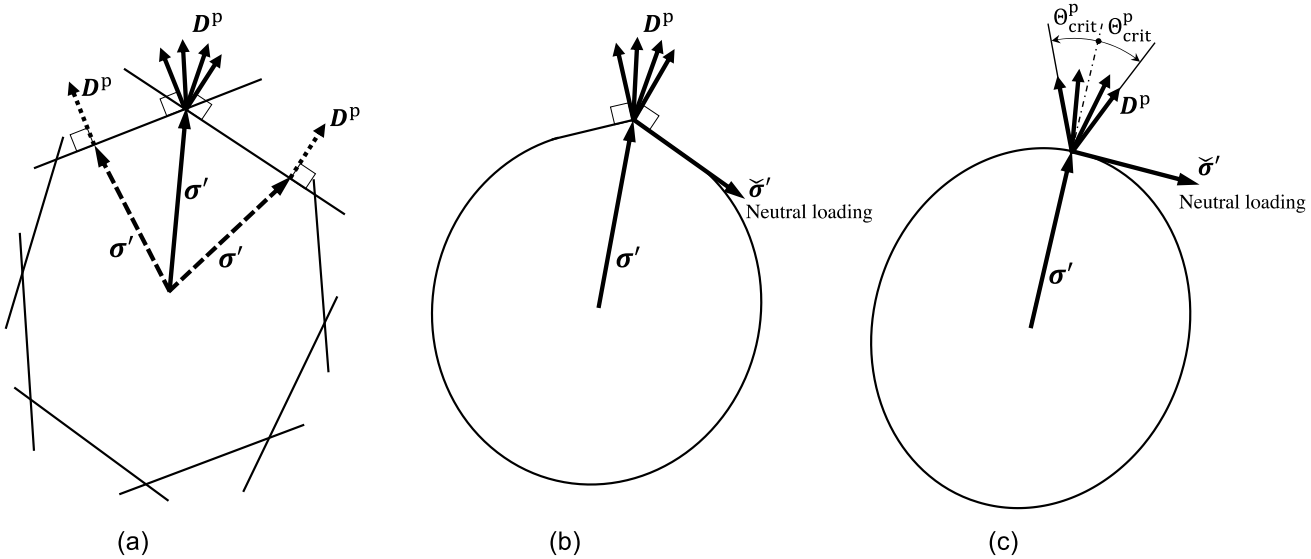

Fig. 1 Schematic illustrations of corners on the yield surface: (**a**) single crystal; (**b**) polycrystal or phenomenological corner theory of plasticity; (**c**) phenomenological *pseudo*-corner theory of plasticity. $\boldsymbol{D}^p$, $\boldsymbol{\sigma}'$ and $\breve{\boldsymbol{\sigma}}'$ are the plastic strain rate, deviatoric stress and stress rate, respectively

the remainder saw smooth yield surfaces. Kuwabara et al. [27] directly detected, for the first time, corners on the yield surfaces of actual polycrystalline metal sheets (an aluminum alloy and a mild steel) using a method proposed by Kuroda and Tvergaard [9], in which first, a specimen is loaded into plastic range, second, at an arbitrary moment, the direction of strain rate is abruptly changed to a significantly different direction (to the extent that elastic unloading is not reached), and then the stress point automatically traces the current yield surface. By this method, we can know the shape of the current yield surface in the vicinity of the loading point without elastic unloading. The effects of the corners, whose existence is obvious in single crystals, persistently remain in polycrystals [1, 2, 27]. Figure 1(b) illustrates schematically a corner on the yield surface of a *polycrystal*, and this also illustrates a conceptual picture of a phenomenological corner theory of plasticity. Figure 1(c) illustrates a concept of a pseudo-corner theory in which modeling of a realistic corner is omitted for simplicity, but a corner-*like* behavior is described by a *non-normality* flow rule on a smooth yield surface [13, 16]. The most marked difference between the real corner [11, 12] and pseudo-corner [13, 16, 17] theories is the direction of the stress rate at a neutral loading state. In the full-scale corner theories, plastic straining continues to occur for the stress rate direction beyond 90° to the full loading direction. The mathematical representation of this behavior tends to be complex [11, 12]. Kuroda and Tvergaard [28] showed that the pseudo-corner theory [16] predicts shear band development similar to that predicted by the corner theory [11] depending on the parameters chosen. Furthermore, phenomenological corner theories (including the pseudo-corner ones) are classified into two groups from another point of view, i.e., the stress rate direction-dependent type [10–12, 14] and strain rate direction-dependent type [13, 16, 17]. When we consider a *nonhardening* material, the stress rate direction is always oriented at a direction tangential to the yield surface regardless of the directions of the strain rate and plastic strain rate. In this regard, the strain rate direction-dependent-type formulation seems to be more reasonable and flexible than the stress rate direction-dependent one.

Most corner theories (including the pseudo-corner ones) [11–13, 15] are extensions of J_2 plasticity in which isotropy is premised. As demonstrated in [16, 29, 30], plastic anisotropy could easily be introduced at least into pseudo-corner theories.

Plastic flow localization analysis

Finite element analysis

Shear band formation in single crystals under plane strain tension was first simulated for a rate-independent material [31] and for a rate-dependent material [24] employing an idealized planar double slip model. Zikry and Nemat-Nasser [32] investigated shear band formation in an FCC single crystal subjected to plane-strain tension at high strain rates. Harren et al. [33] studied shear band formation in plane-strain compression of single crystals and polycrystals. Watanabe et al. [34] carried out computations of shear band development in polycrystals numerically generated with a Voronoi tessellation technique using different types of finite element. Inal et al. [35, 36] presented plastic flow localization in FCC polycrystals (described by the Taylor model [7]) subjected to tension both under plane strain [35] and plane stress [36] conditions. Kuroda and Tvergaard [28] simulated shear band development in FCC and BCC polycrystals subjected to plane strain tension. In the examples referred above, natural consequences of the vertex effect with respect to plastic flow localization were well documented.

Another attractive characteristic inherent in the crystal plasticity model is the capability for natural description of initial anisotropy and its subsequent evolution. Kuroda and Tvergaard [37] investigated shear band formation in textured FCC polycrystalline sheets subjected to tension/compression and pure bending under plane strain conditions and showed that the cube texture has extremely high resistance to shear band formation. Ikawa et al. [38] compared FE and experimental results of bending tests on aluminum alloy (A6061-T4) sheets having Goss and cube orientations. Figure 2 shows shear band developments in bent specimens [38]. The finite element results well reproduced the experimental results with particular focus on the extremely low resistance to shear band formation of Goss texture in transvers direction (TD) bending ($\Phi = 90^{\circ}$). The Goss texture is known to have marked anisotropy, which shows almost no indication of shear band formation in rolling direction (RD) bending ($\Phi = 0^{\circ}$).

The capability of the phenomenological corner theory [11] to predict plastic flow localization was demonstrated for plane strain tension [21] and pure bending [39]. In [40], severely nonuniform deformation near a blunted crack tip under the mode I loading condition was predicted. In [28], it was demonstrated that computations with the pseudo-corner theory [16] well reproduce the shear band development behavior predicted by polycrystal plasticity computations. In [30], shear band development in anisotropic bent specimens was analyzed using the pseudo-corner theory [16] combined with Hill's yield function [41]. In [42], the pseudo-corner theory [16] was extended to incorporate hydrostatic stress sensitivity and showed that the hydrostatic stress sensitivity hastens the development of diffuse neck and shear band formation in plane strain tension. Recently, Yoshida [17] simulated shear band development in plane strain tension and bending using his newly proposed pseudo-corner theory.

Regarding finite elements, constant strain triangular elements in the form of 'crossed triangles' were frequently used in early plastic flow localization analyses, which

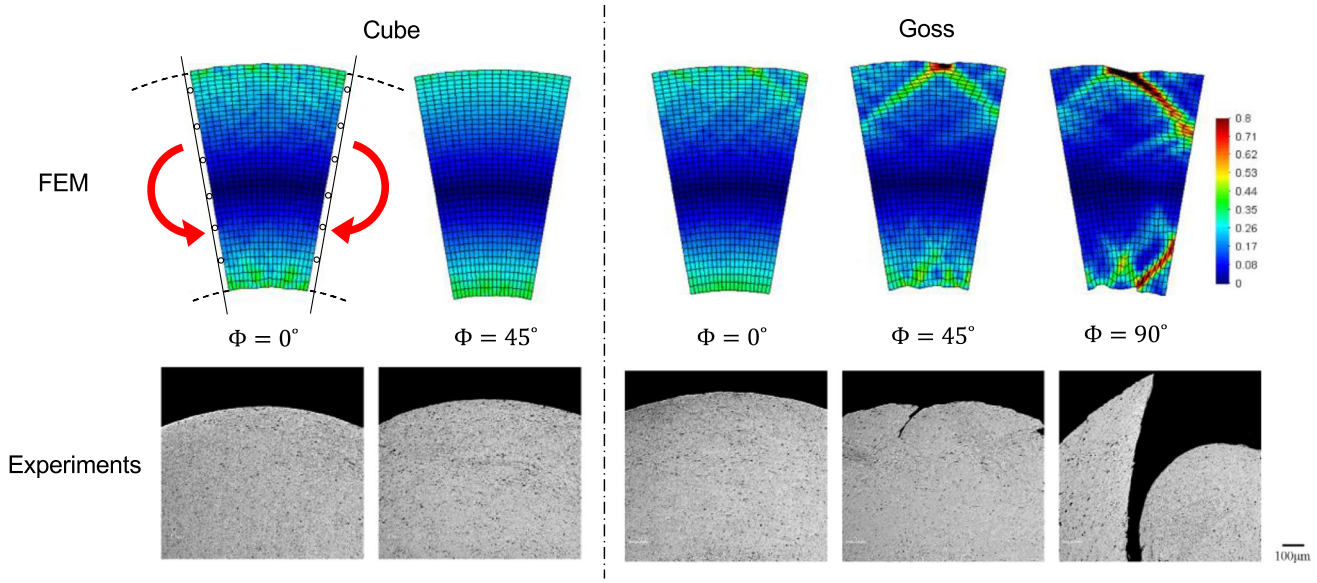

Fig. 2 Shear band development in bent specimens. Results of crystal plasticity finite element computations and corresponding experiments on an A6061-T4 aluminum alloy sheet [38] with cube and Goss orientations. Φ denotes an angle of the cutting direction of bending specimens relative to RD. In finite element analysis, an initially rectangular block under plane strain conditions, which models a part of a long sheet, was subjected to pure bending. Crystal orientations randomly selected from ODF (orientation distribution function) data determined with measured pole figures were allocated for Gaussian integration points. Color contours represent distribution of maximum principal logarithmic strain

require a proper design with respect to mesh orientation [21]. In [43], it was shown that the serendipity quadratic element with reduced integration provides relatively favorable solutions for strain localization problems.

Simplified analysis

One of the most important engineering applications of plastic flow localization analysis is the quantitative evaluation of the limits to the ductility of sheet metals subjected to biaxial stretching, i.e., the depiction of *forming limit diagrams* (FLDs). For this purpose, full-field analyses with the direct use of the finite element method have not been widely used. The Marciniak–Kuczynski (MK) [44] technique has been the most popular method for the evaluation of sheet metal formability. In this approach, two homogeneously deforming regions (elements) are considered. One region is assumed to have an initial thickness slightly smaller than that of the other. This thickness difference acts as a geometrical imperfection that progressively evolves until plastic flow localization (i.e., sheet necking) occurs in the thinner region accompanying the occurrence of elastic unloading in the thicker region. The MK approach is fairly simple, but is very efficient for industrial applications.

In the MK approach, the equilibrium and compatibility of the two elements are described by

$$\boldsymbol{n} \bullet \boldsymbol{\sigma}^{\mathrm{b}} h^{\mathrm{b}} = \boldsymbol{n} \bullet \boldsymbol{\sigma}^{\mathrm{o}} h^{\mathrm{o}}, \tag{1}$$

$$\boldsymbol{L}^{\mathrm{b}} = \boldsymbol{L}^{\mathrm{o}} + \dot{\boldsymbol{c}} \otimes \boldsymbol{n}. \tag{2}$$

Here, $\boldsymbol{n}$ is the current unit normal vector to the interface between the two elements, $\boldsymbol{\sigma}$ is the Cauchy stress, $\boldsymbol{L}$ is the velocity gradient, h is thickness, superscripts 'b' and 'o' represent the places where the corresponding quantity is defined (that is, the thinner region is denoted by 'b' because it is often also referred to as the imperfection *band* region and the thicker region is denoted by 'o' because it is often also referred to as the region *outside* the band) and $\dot{\boldsymbol{c}}$ is the vector quantity to be determined. Equations (1) and (2) together with the constitutive model employed result in the following form of simple algebraic equations for the vector quantity $\dot{\boldsymbol{c}}$ (e.g., [45]):

$$\begin{pmatrix} a_{11} & a_{12} \\ a_{21} & a_{22} \end{pmatrix} \begin{Bmatrix} \dot{c}_1 \\ \dot{c}_2 \end{Bmatrix} = \begin{Bmatrix} b_1 \\ b_2 \end{Bmatrix} D_{11}, \tag{3}$$

where D_{11} is the strain rate component in the major strain direction. Strictly speaking, plastic flow localization is said to occur when elastic unloading (strain rate reversal) takes place in the thicker region causing the plastic flow to concentrate in the thinner region. In the literature, however, D_{11} is mostly used as a prescribed quantity [46] so that elastic unloading in the thicker region never occurs. The onset of sheet necking is approximated by the occurrence of a much

higher strain rate in the thinner region than in the thicker region. In order to detect precisely the occurrence of elastic unloading in the thicker region (i.e., detection of the moment at which D_{11} changes its sign), the prescribed quantity must be switched from D_{11} to $\dot{c}_1$ or $\dot{c}_2$ at a certain stage of deformation. In this way, we are able to know the exact point of the onset of sheet necking and continue the computation into the *post-localization* region. This technique may be needed in cases where strain path changes, which often cause *pseudo-localization* behavior followed by the reappearance of a stable deformation state, are considered [45]. In order to judge whether the real localization that never ceases occurs or not, precise detection of the change in the sign of D_{11} is required. The detailed procedure is described in [45].

If we consider no imperfection, the MK approach coincides with a bifurcation analysis. In this case, the right-hand side of Eq. (3) becomes a zero vector, and thus, the condition $\det[a] = 0$ is the condition for a nontrivial solution of $\dot{\boldsymbol{c}}$. The prediction of forming limit strains by the bifurcation approach is extremely sensitive to the constitutive model employed, particularly in the biaxial stretching range. Classical theories of plasticity based on a smooth yield surface and the normality flow rule give bifurcation solutions at an unrealistic stress level as large as the order of the elastic modulus, whereas the J_2-deformation theory [10], which is the basis of the J_2-corner theory [11], predicts a bifurcation solution at realistic stress and strain levels. The crystal plasticity theory also predicts realistic bifurcation solutions, as shown in [47, 48]. It has been shown in [48] that a geometrical imperfection ξ_I of 10^{-4} gives a FLD indistinguishable from that predicted by the bifurcation analysis for both the cases of the J_2-deformation theory and crystal plasticity theory, where $\xi_I = 1 - h_I^b/h_I^o$ with h_I^b and h_I^o being the initial thicknesses in the thin and thick regions, respectively. Figure 3(a) shows FLDs computed with the MK and bifurcation approaches for the J_2-deformaiton theory and J_2-flow (normality) theory, and Fig. 3(b) shows FLDs for the crystal plasticity theory. Note that the J_2 flow (normality) theory exhibits a strong dependence on the imperfection, and an imperfection ξ_I of 10^{-4} gives unrealistically high limit strains. Tvergaard [49] showed that the introduction of a kinematic hardening rule results in much smaller limit strains than those predicted by the isotropic hardening J_2-flow theory (employed in Fig. 3(a)), and this might be interpreted as representing a smooth yield surface that develops a sort of rounded vertex on the loading point with a local curvature equal to that of the initial yield surface.

It is emphasized that the bifurcation approach has a serious limitation preventing its practical application to engineering materials. When the material rate dependence (i.e., viscosity) is introduced in the constitutive model, the bifurcation solution is solely governed by the elastic moduli. In general, all real materials have a rate dependence that has significant effects on limit strains and plastic flow localization behavior [16, 50]. In this regard, the imperfection (MK) approach has much wider applicability than the bifurcation approach, bearing in mind that the constitutive model employed should involve the corner (or pseudo-corner) effects; otherwise, MK solutions highly depend on the imperfection value assumed and this may not be physically acceptable.

In using crystal plasticity model in the MK approach, an important issue is what type of homogenization method is efficient and accurate for representing the overall behavior of the polycrystalline aggregate under consideration. There are mainly three choices: (i) the classical Taylor model in which strains in each crystal grain are uniform and are assumed to be identical to the overall strain of the aggregate [7], (ii) the self-consistent approach [2, 25, 51–54], and (iii) the homogenization-based polycrystal finite element method [55]. The accuracy of the prediction of sheet necking in the MK approach, as well as in the bifurcation approach, depends on the accuracy of the predicted values of overall (homogenized) stress and hardening modulus. In

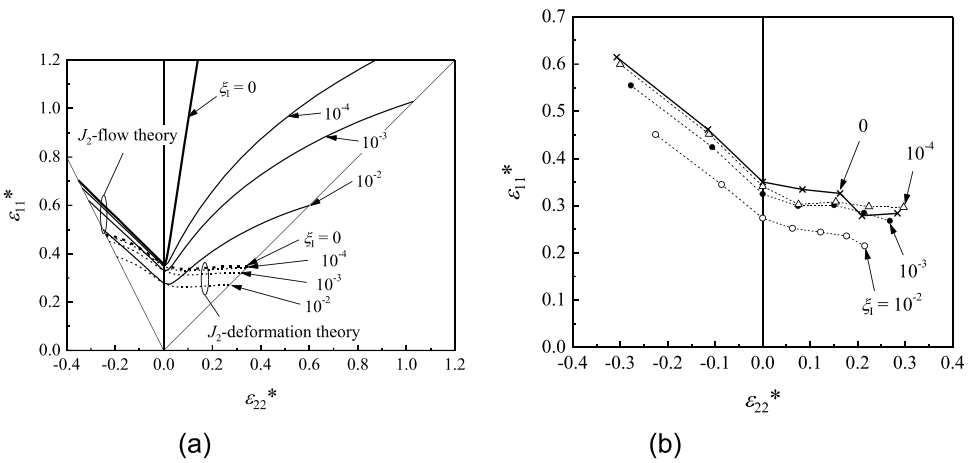

Fig. 3 Effects of geometrical imperfection on forming limit strains [48]: (**a**) J_2-deformation and J_2-flow theories; (**b**) rate-independent crystal plasticity model with random texture (the Taylor model was adopted for representing homogenized polycrystal behavior). In all the computations, power-law hardening with an exponent of 0.35 is assumed

[56], the geometrical hardening behavior owing to texture evolution in FCC polycrystals was investigated, and it was shown that the classical Taylor model exhibits almost the same macroscopic hardening behavior as those predicted by the homogenization-based polycrystal finite element method, at least for a cube texture material and for a material with a particular texture that leads to very high geometrical hardening. A quantitative reexamination of the Taylor model for FCC polycrystals via the homogenization-based polycrystal finite element method was reported in [57]. The Taylor model was used in MK analyses in [16, 48, 56, 58–64]. Tadano et al. [65] showed that the Taylor model and the homogenization-based polycrystal finite element method yield almost the same FLD, at least for random and cube textured FCC sheets. Lebensohn et al. [54] and Signorelli et al. [66] used the MK technique coupled with the self-consistent models. Signorelli and co-workers [67–69] showed that the Taylor model does not necessarily result in realistic FLDs, depending on the texture and crystal structure, whereas the viscoplastic self-consistent model gives FLDs consistent with experimental results. Theoretically, the most reliable model among the three is the homogenization-based polycrystal finite element method, which satisfies both equilibrium and compatibility between grains in the aggregate. The MK-self-consistent approach should be subject to further investigation via comparison with the homogenization-based polycrystal finite element method in the future. A schematic illustration of the MK technique combined with the homogenization-based polycrystal finite element method, which was originally proposed by Tadano et al. [65], is shown in Fig. 4. This method is expected to be efficient for forming limit predictions not only of polycrystals, but also of voided (damaged), multiphase and/or composite (particle reinforced) materials. Very recently, the MK technique in conjunction with crystal plasticity models have been comprehensively reviewed by Signorelli et al. [46].

The fundamental idea of the MK technique can also be applied to a simplified three-dimensional analysis of shear band formation in a bulk material. Details and applications can be found in [18, 37, 70].

Width of plastic flow localization region – strain gradient plasticity–

Classical plasticity theories (including crystal plasticity theories) do not include any intrinsic material length-scale effects. This could be a drawback in plastic flow localization analysis since shear band width is not determined as a finite size. When we perform finite element analysis including shear band formation, the shear band width becomes narrower and narrower as the finite element mesh is refined. In other words, the shear band width unreasonably coincides with the size of one finite element, and thus, mesh convergence is not reached. Strain gradient plasticity theories aim to represent the material length-scale effects inherent in actual materials.

Strain gradient plasticity (SGP) theories are classified into three types. One type of theory, proposed by Acharya and Bassani [71] retains conventional stresses, equilibrium equations and boundary conditions, but incorporates a dependence on plastic strain gradients into incremental tangential hardening moduli. The second type of theory is that first proposed by Aifantis [72] in which higher-order spatial gradients of plastic strain are introduced into the yield function. In addition to changing the constitutive relation, an extra governing differential equation is introduced along with additional (microscopic) boundary conditions (e.g., Mühlhaus and Aifantis [73]; Zbib and Aifantis [74];

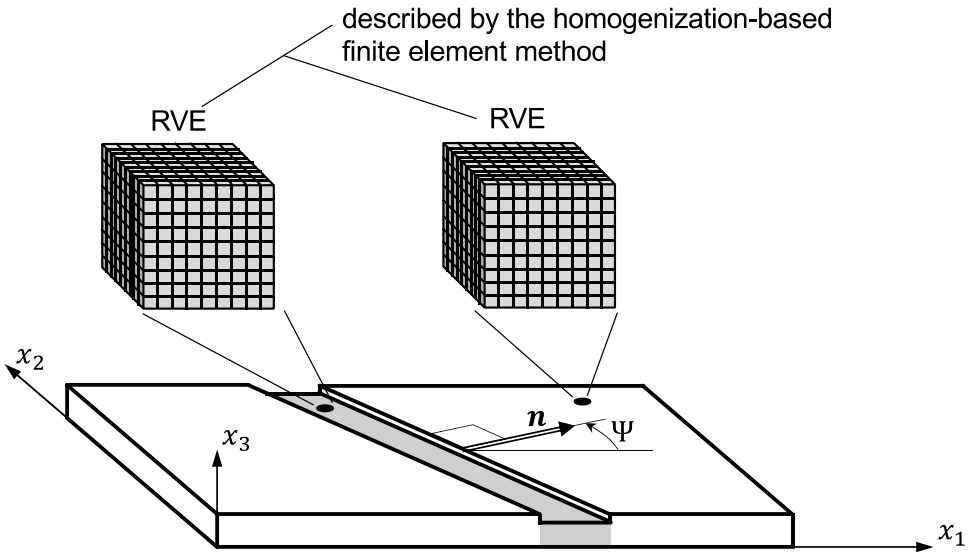

Fig. 4 Marciniak–Kuczynski technique combined with homogenization-based finite element method [65]. Two regions with slightly different thicknesses are modeled by initially identical representative volume elements (RVEs)

de Borst et al. [75]; Fleck and Hutchinson [76]; Gurtin and Anand [77]; Fleck et al. [78]). Introduction of higher-order plastic strain gradient effects results in unique solutions to problems involving plastic flow localization phenomena. The third type of theory is the class of higher-order theories proposed by Fleck and Hutchinson [79] in which the gradients of the total strains are introduced as a third-order tensor and the gradient effect emerges even when the deformations are elastic. Recent years, the second type is most widely accepted for microscale plasticity computations. In the present study, the second type will be featured.

Aifantis [72] proposed that higher-order spatial gradients of plastic strain be introduced into the conventional yield function:

$$\sigma_{\mathrm{e}} + \nabla \bullet \boldsymbol{g}^{\mathrm{p}} - R(\varepsilon^{\mathrm{p}}) = 0, \tag{4}$$

$$\boldsymbol{g}^{\mathrm{p}} = \beta \nabla \varepsilon^{\mathrm{p}}, \tag{5}$$

where σ_{e} is an equivalent stress, β is a length-scale coefficient having a dimension of force that is often assumed to be $\beta = l^2\sigma_0$ with l and σ_0 being a length scale and a reference stress, respectively, ε^{p} is an equivalent plastic strain, ∇ is a spatial gradient operator (nabla), and $R(\varepsilon^{\mathrm{p}})$ is a strain hardening function. With the introduction of the spatial gradient term, the yield function acquires the nature of a partial differential equation. This is not only a change of the constitutive relation, but also an introduction of an additional governing equation with concomitant unconventional boundary conditions. Equation (4) with Eq. (5) is one of the simplest models [72]. More elaborate relations can be found in the literature [76, 80, 81]. The weak form of an incremental form of Eq. (4) is written as

$$\int_V \left\{ \left(\dot{R} - \dot{\sigma}_{\mathrm{e}} \right) \delta\dot{\varepsilon}^{\mathrm{p}} + \dot{\boldsymbol{g}}^{\mathrm{p}} \bullet \nabla \delta\dot{\varepsilon}^{\mathrm{p}} \right\} \mathrm{d}V = \int_S \overline{\boldsymbol{n}} \bullet \dot{\boldsymbol{g}}^{\mathrm{p}} \delta\dot{\varepsilon}^{\mathrm{p}} \mathrm{d}S, \tag{6}$$

where $\delta\dot{\varepsilon}^{\mathrm{p}}$ is an arbitrary weighting function that can be viewed as a virtual plastic strain rate, V and S are the volume and surface of the body and $\overline{\boldsymbol{n}}$ is a unit normal vector to $\mathrm{d}S$. We can prescribe values of $\overline{\boldsymbol{n}} \bullet \dot{\boldsymbol{g}}^{\mathrm{p}}$ or $\dot{\varepsilon}^{\mathrm{p}}$ on S as extra (higher-order) boundary conditions. In principle, this additional governing equation should be solved simultaneously with the conventional force equilibrium equation. The system of finite element equations takes the form [73, 75, 82, 83]

$$\begin{bmatrix} \boldsymbol{K}_{(\mathrm{uu})} & \boldsymbol{K}_{(\mathrm{up})} \\ \boldsymbol{K}_{(\mathrm{pu})} & \boldsymbol{K}_{(\mathrm{pp})} \end{bmatrix} \begin{Bmatrix} \dot{\boldsymbol{U}} \\ \dot{\boldsymbol{\epsilon}}^{\mathrm{p}} \end{Bmatrix} = \begin{Bmatrix} \dot{\boldsymbol{F}}_{(\mathrm{u})} \\ \dot{\boldsymbol{F}}_{(\mathrm{p})} \end{Bmatrix}, \tag{7}$$

where $\{\dot{\boldsymbol{U}}\}$ is a vector array of nodal displacement rates and $\{\dot{\boldsymbol{\epsilon}}^{\mathrm{p}}\}$ is that of nodal equivalent plastic strain rates. The first and second rows of Eq. (7) are derived from the standard virtual work relation (the force equilibrium relation) and Eq. (6), respectively. Discussions on a variety of treatments of strain gradient plasticity and related issues on numerical analysis have been given in [84, 85].

The introduction of the higher-order strain gradient effects revives the uniqueness of the solution for problems accompanying plastic flow localization. Early pioneering studies (e.g., [74, 75]) on plastic flow localization with the size effect mainly considered strain-softening solids. These studies showed that the severe mesh dependence is remedied with the introduction of the strain gradient effects. Recently, a pseudo-corner theory of plasticity [16] was incorporated into the framework of strain gradient plasticity [82, 83]. Figure 5 shows the results of a plane strain tension problem involving shear band formation with and without material length-scale (strain gradient) effects. The shear band width depends on the mesh discretization in the case of the conventional size-independent theory, whereas the strain gradient theory predicts an identical shear band width regardless of mesh design. The gradient term $\nabla \bullet \boldsymbol{g}^{\mathrm{p}}$ works to augment stresses as seen in the distribution of $\sigma_{\mathrm{e}}/\sigma_0$ in Fig. 5. This leads to a delay of strain localization.

In [86, 87], the strain gradient plasticity theory was combined with the MK technique. In this approach, the neck profile and the corresponding deformation state inside and outside the neck region can be determined using a numerical scheme based on the strain gradient theory. It was reported that the gradient plasticity theory significantly reduces the imperfection sensitivity encountered in the conventional MK approach [86, 87].

For single crystals, several gradient theories have also been proposed. Gurtin [88, 89] presented a higher-order gradient crystal plasticity theory based on an extended virtual work principle that involves unconventional *higher-order stresses* whose constitutive relations are derived in a thermodynamically consistent manner. Groma et al. [90], Yefimov et al. [91], Evers et al. [92] and Bayley et al. [93] independently proposed a different type of gradient theory whose primal component is a backstress (equivalent to an internal stress with the opposite sign) arising in response to spatial gradients of density of geometrically necessary dislocations (GNDs), which corresponds to the first-order spatial gradient of crystallographic slip. It has been shown that fundamentally, these two different types of gradient crystal plasticity theory are mathematically equivalent and give the same solution for the same boundary value problem [94–96]. The simplest yield condition for a slip system can be written as

$$\tau^{(\alpha)} + \nabla \bullet \boldsymbol{\xi}^{(\alpha)} - g^{(\alpha)} = 0, \tag{8}$$

$$\boldsymbol{\xi}^{(\alpha)} = -\beta^{(\alpha)} \left(\rho^{(\alpha)}_{\mathrm{G(e)}} \boldsymbol{s}^{(\alpha)} + \rho^{(\alpha)}_{\mathrm{G(s)}} \boldsymbol{p}^{(\alpha)} \right), \tag{9}$$

where $\tau^{(\alpha)}$ is the resolved shear stress on slip system α, $g^{(\alpha)}$ is slip resistance, $\rho^{(\alpha)}_{\mathrm{G(e)}}$ and $\rho^{(\alpha)}_{\mathrm{G(s)}}$ are the edge and screw GND densities, $\boldsymbol{s}^{(\alpha)}$ is the slip direction, $\boldsymbol{p}^{(\alpha)}$ is the tangent line

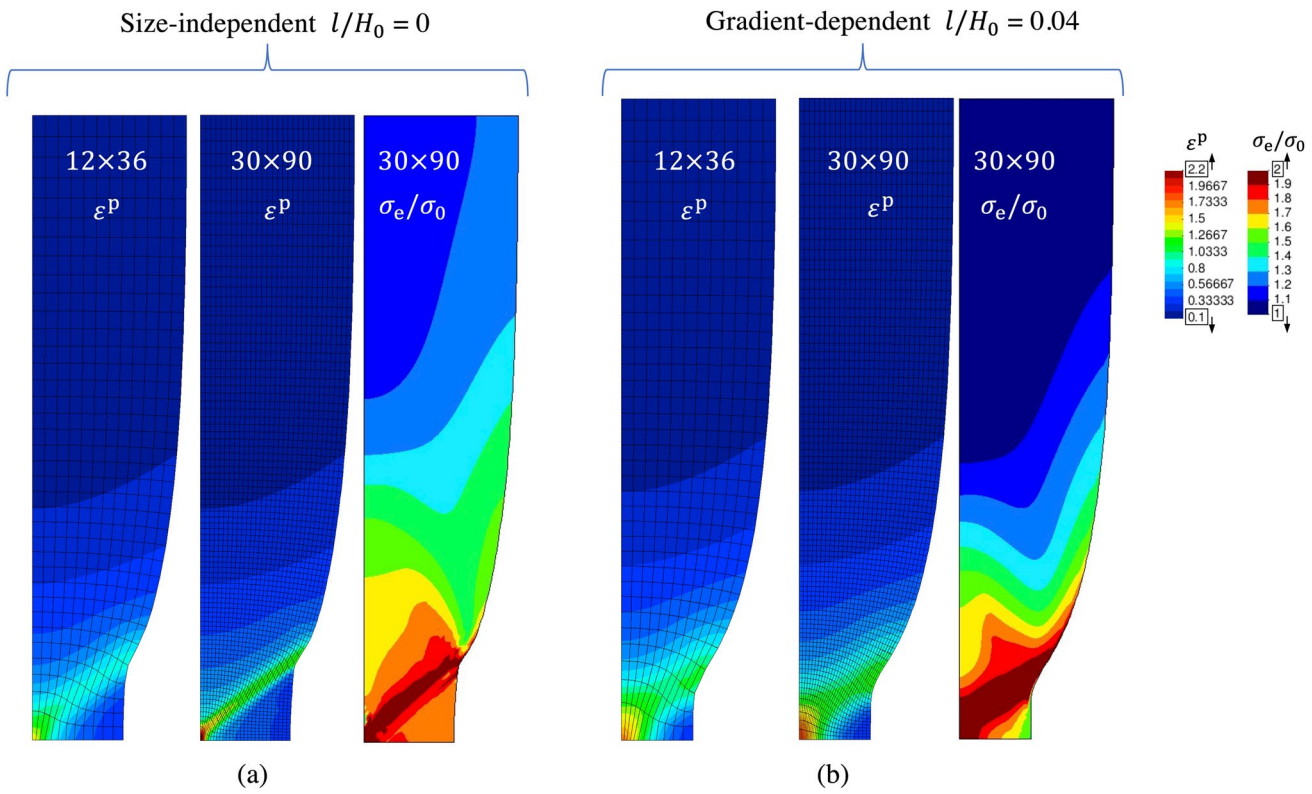

Fig. 5 Shear band formation in plane strain tension predicted by pseudo-corner theory of plasticity [82]: **a** Conventional size-independent computations ($l/H_0 = 0$) and (**b**) strain gradient plasticity computations ($l/H_0 = 0.04$). For each case, distributions of ε^p for coarse mesh (12×36 quadrilateral elements) and fine mesh (30×90 quadrilateral elements), and distribution of σ_e/σ_0 for the fine mesh are displayed. A quarter portion of a rectangular-shaped specimen with a width of $2H_0$ under plane strain conditions was analyzed with introduction of symmetric boundary conditions and small geometric imperfections to trigger off diffuse necking

direction of edge dislocations and $\beta^{(\alpha)}$ is a coefficient associated with the length-scale. Equation (8) with Eq. (9) is one of the simplest models in the Gurtin-type approach [88, 89]. The term $\nabla \bullet \boldsymbol{\xi}^{(\alpha)}$ can be viewed as a backstress ($\tau_b^{(\alpha)}$) in the alternative approach [90–93]. If the correlation $\tau_b^{(\alpha)} = \nabla \bullet \boldsymbol{\xi}^{(\alpha)}$ holds, the two approaches can be mathematically equivalent. More elaborate relations for $\boldsymbol{\xi}^{(\alpha)}$ and $\tau_b^{(\alpha)}$ can be found in the literature (e.g., [88, 89, 92, 93]). Applications of higher-order gradient crystal plasticity have been reported in [97–102]. Similar to the phenomenological strain gradient theories, the gradient crystal plasticity theories eliminate the mesh dependence in finite element simulations of plastic flow localization problems (e.g., [97, 102, 103]).

Concluding remarks

When a normality flow rule with a smooth yield surface is assumed, a change in the direction of plastic strain rate requires a corresponding amount of change in the total stress direction. This inhibits abrupt change in the deformation mode and prevents the occurrence of plastic flow localization. The corner theories of plasticity (including the pseudo ones) naturally overcome this difficulty. When the early corner theories [10–13, 23] were proposed, the existence of the corners in practical polycrystalline metals was not proved experimentally, but they were based on the conceptual need for the corners. The existence of the corners was proved by Kuwabara et al. [27], and now, we can employ the corner theories as ones that have a firm physical background. The crystal plasticity theory inherently possesses the vertex effect and automatically represents plastic flow localization without any additional consideration if its occurrence is a physical necessity. Furthermore, the crystal plasticity theory is capable of representing the initial anisotropy using the measured crystal orientation distribution and pursuing its subsequent evolution. This clearly exceeds the corresponding potential capability in phenomenological corner theories.

Declarations

Conflict of interest The author declares that he has no conflict of interest.

References

1. Hill R (1967) The essential structure of constitutive laws for metal composites and polycrystals. J Mech Phys Solids 15:79–95
2. Hutchinson JW (1970) Elastic-plastic behavior of polycrystalline metals and composites. Proc Roy Soc Lond A319:247–272
3. Gurson AL (1977) Continuum theory of ductile rupture by void nucleation and growth-I. yield criteria and flow rules for porous ductile media. ASME J Eng Mater Technol 99:2–15
4. Tvergaard V (1987) Effect of yield surface curvature and void nucleation on plastic flow localization. J Mech Phys Solids 35:43–60
5. Wright TW, Batra RC (1985) The initiation and growth of adiabatic shear bands. Int J Plast 1:205–212
6. Spitzig WA, Sober RJ, Richmond O (1975) Pressure dependence of yielding and associated volume expansion in tempered martensite. Acta Metall 23:885–893
7. Taylor GI (1938) Plastic strain in metals. J Inst Metals 62:307–324
8. Asaro RJ (1979) Geometrical effects in the inhomogeneous deformation of ductile single crystals. Acta Metall 27:445–453
9. Kuroda M, Tvergaard V (1999) Use of abrupt strain path change for determining subsequent yield surface: illustrations of basic idea. Acta Mater 47:3879–3890
10. Støren S, Rice JR (1975) Localized necking in thin sheets. J Mech Phys Solids 23:421–441
11. Christoffersen J, Hutchinson JW (1979) A Class of Phenomenological Corner Theories of Plasticity. J Mech Phys Solids 27:465–487
12. Gotoh M (1985) A simple plastic constitutive equation with vertex effect. Eng Fract Mech 21:673–684
13. Simo JC (1987) A J2-flow theory exhibiting a corner-like effect and suitable for large-scale computation. Comput Methods Appl Mech Eng 62:169–194
14. Ito K, Satoh K, Goya M, Yoshida T (2000) Prediction of limit strain in sheet metal-forming processes by 3D analysis of localized necking. Int J Mech Sci 42:2233–2248
15. Hughes TR, Shakib F (1986) Pseudo-corner theory: a simple enhancement of J2-flow theory for applications involving non-proportional loading. Eng Comput 3:116–120
16. Kuroda M, Tvergaard V (2001) A phenomenological plasticity model with non-normality effects representing observations in crystal plasticity. J Mech Phys Solids 49:1239–1263
17. Yoshida Y (2017) A plastic flow rule representing corner effects predicted by rate-independent crystal plasticity. Int J Solids Struct 120:213–225
18. Hutchinson JW, Tvergaard V (1981) Shear band formation in plane strain. Int J Solids Struct 17:451–470
19. McMeeking RM, Rice JR (1975) Finite-element formulations for problems of large elastic-plastic deformation. Int J Solids Struct 11:601–616
20. Burke MA, Nix WD (1979) A numerical study of necking in the plane tension test. Int J Solids Struct 15:379–393
21. Tvergaard V, Needleman A, Lo KK (1981) Flow localization in the plane strain tensile test. J Mech Phys Solids 29:115–142
22. Sewell MJ (1974) A plastic flow rule at a yield vertex. J Mech Phys Solids 22:469–490
23. Hutchinson JW (1974) Plastic buckling. Adv Appl Mech (ed. C.S. Yih) 14: 67–144.
24. Peirce D, Asaro RJ, Needleman A (1983) Material rate dependence and localized deformation in crystalline solids. Acta Metall 31:1951–1976
25. Hill R (1965) Continuum micro-mechanics of elasto-plastic polycrystals. J Mech Phys Solids 13:89–101
26. Hecker SS (1976) Experimental studies of yield phenomena in biaxially loaded metals. In: Stricklin JA, Saczalski KH (eds) Constitutive Equations in Viscoplasticity: Computational and Engineering Aspects. ASME, New York, pp 1–33
27. Kuwabara T, Kuroda M, Tvergaard V, Nomura K (2000) Use of abrupt strain path change for determining subsequent yield surface: Experimental study with metal sheets. Acta Mater 48:2071–2079
28. Kuroda M, Tvergaard V (2001) Shear band development predicted by a non-normality theory of plasticity and comparison to crystal plasticity predictions. Int J Solids Struct 38:8945–8960
29. Kuroda M, Tvergaard V (2001) Plastic spin associated with a non-normality theory of plasticity. Eur J Mech A/Solids 20:893–905
30. Kuroda M, Tvergaard V (2004) Shear band development in anisotropic bent specimens. Eur J Mech A/Solids 23:811–821
31. Peirce D, Asaro RJ, Needleman A (1982) An analysis of nonuniform and localized deformation in ductile single crystals. Acta Metall 30:1087–1099
32. Zikry MA, Nemat-Nasser S (1990) High strain-rate localization and failure of crystalline materials. Mech Mater 10:215–237
33. Harren SV, Deve HE, Asaro RJ (1988) Shear band formation in plane strain compression. Acta Metall 9:2435–2480
34. Watanabe O, Zbib HM, Takenouchi E (1998) Crystal plasticity: micro-shear banding in polycrystals using Voronoi tessellation. Int J Plast 14:771–788
35. Inal K, Wu PD, Neale KW (2002) Instability and localized deformation in polycrystalline solids under plane-strain tension. Int J Solids Struct 39:983–1002
36. Inal K, Wu PD, Neale KW (2002) Finite element analysis of localization in FCC polycrystalline sheets under plane stress tension. Int J Solids Struct 39:3469–3486
37. Kuroda M, Tvergaard V (2007) Effects of texture on shear band formation in plane strain tension/compression and bending. Int J Plast 23:244–272
38. Ikawa S, Asano M, Kuroda M, Yoshida K (2011) Effects of crystal orientation on bendability of aluminum alloy sheet. Mater Sci Eng A528:4050–4054
39. Triantafyllidis N, Needleman A, Tvergaard V (1982) On the development of shear bands in pure bending. Int J Solids Struct 18:121–138
40. Needleman A, Tvergaard V (1983) Crack-tip stress and deformation fields in a solid with a vertex on its yield surface. Elastic-Plastic Fracture: Second Symposium, Volume I–Inelastic Crack Analysis. In: Shih CF, Gudas JP (Eds.) ASTM STP 803, American Society for Testing and Materials, pp. I-80–I-115
41. Hill R (1948) A theory of the yielding and plastic flow of anisotropic metals. Proc Roy Soc Lond A193:281–297
42. Kuroda M (2004) A phenomenological plasticity model accounting for hydrostatic stress-sensitivity and vertex-type of effect. Mech Mater 36:285–297
43. Mathur KK, Needleman A, Tvergaard V (1994) Ductile failure analyses on massively parallel computers. Comput Meth Appl Mech Eng 119:283–309
44. Marciniak Z, Kuczynski K (1967) Limit strains in the processes of stretch-forming sheet metal. Int J Mech Sci 9:609–620
45. Kuroda M, Tvergaard V (2000) Effect of strain path change on limits to ductility of anisotropic metal sheets. Int J Mech Sci 42:867–887

46. Signorelli JW, Bertinetti MA, Roatta A (2021) A review of recent investigations using the Marciniak-Kuczynski technique in conjunction with crystal plasticity models. J Mater Process Technol 287:116157
47. Knockaert R, Chastel Y, Massoni E (2000) Rate-independent crystalline and polycrystalline plasticity, application to FCC materials. Int J Plast 16:179–198
48. Yoshida K, Kuroda M (2012) Comparison of bifurcation and imperfection analyses of localized necking in rate-independent polycrystalline sheets. Int J Solids Struct 49:2073–2084
49. Tvergaard V (1980) Bifurcation and imperfection-sensitivity at necking instabilities. ZAMM 60:T26–T34
50. Hutchinson JW, Neale KW (1978) Sheet necking - III. Strain rate effects. In: Koistinen, DP, Wang N-M (Eds.), Mechanics of Sheet Metal Forming. Plenum Publ. Corp., New York, pp. 269–285
51. Iwakuma T, Nemat-Nasser S (1984) Finite elastic-plastic deformation of polycrystalline metals. Proc Roy Soc Lond A394:87–119
52. Nemat-Nasser S, Obata M (1986) Rate-dependent finite elasto-plastic deformation of polycrystals. Proc Roy Soc Lond A407:343–375
53. Molinari A, Canova GR, Ahzi S (1987) A self-consistent approach of the large de- formation polycrystal viscoplasticity. Acta Metall 35:2983–2994
54. Lebensohn RA, Tomé CN (1993) A self-consistent approach for the simulation of plastic deformation and texture development of polycrystals: application to Zr alloys. Acta Metall Mater 41:2611–2624
55. Guedes J, Kikuchi N (1990) Preprocessing and postprocessing for materials based on the homogenization method with adaptive finite element methods. Comput Meth Appl Mech Eng 83:143–198
56. Yoshida K, Tadano Y, Kuroda M (2009) Improvement in formability of aluminum alloy sheet by enhancing geometrical hardening. Comput Mater Sci 46:459–468
57. Tadano Y, Kuroda M, Noguchi H (2012) Quantitative re-examination of Taylor model for FCC polycrystals. Comput Mater Sci 51:290–302
58. Wu PD, Neale KW, Van der Giessen E (1997) On crystal plasticity FLD analysis. Proc Roy Soc Lond A 453:1831–1848
59. Wu PD, Neale KW, Van der Giessen E, Jain M, Makinde A, MacEwen SR (1998) Crystal plasticity forming limit diagram analysis of rolled aluminum sheets. Metall Mater Trans A 29A:527–535
60. Wu PD, MacEwena SR, Lloyd DJ, Neale KW (2004) Effect of cube texture on sheet metal formability. Mater Sci Eng A364:182–187
61. Inal K, Neale KW, Aboutajeddine A (2005) Forming limit comparisons for FCC and BCC sheets. Int J Plast 21:1255–1266
62. Yoshida K, Ishizaka T, Kuroda M, Ikawa S (2007) The effects of texture on formability of aluminum alloy sheets. Acta Mater 55:4499–4506
63. Yoshida K, Kuroda M (2012) Numerical investigation on a key factor in superior stretchability of face-centered cubic polycrystalline sheets. Int J Mech Sci 58:47–56
64. Chiba R, Takeuchi H, Kuroda M, Hakoyama T, Kuwabara T (2013) Theoretical and experimental study of forming-limit strain of half-hard AA1100 aluminium alloy sheet. Comput Mater Sci 77:61–71
65. Tadano Y, Yoshida K, Kuroda M (2013) Plastic flow localization analysis of heterogeneous materials using homogenization-based finite element method. Int J Mech Sci 72:63–74
66. Signorelli JW, Bertinetti MA, Turner PA (2009) Predictions of forming limit diagrams using a rate-dependent polycrystal self-consistent plasticity model. Int J Plast 25:1–25
67. Signorelli JW, Bertinetti MA (2009) On the role of constitutive model in the forming limit of FCC sheet metal with cube orientations. Int J Mech Sci 51:473–480
68. Signorelli JW, Serenelli MJ, Bertinetti MA (2012) Experimental and numerical study imposed hydrostatic pressure on sheet metal formability. Int J Plast 25:1711–1725
69. Serenelli MJ, Bertinetti MA, Signorelli JW (2010) Investigation of the dislocation slip assumption on formability of BCC sheet metals. Int J Mech Sci 52:1723–1734
70. Tvergaard V, Needleman A (1993) Shear band development in polycrystals. Proc Roy Soc Lond A443:547–562
71. Acharya A, Bassani JL (2000) Incompatibility and crystal plasticity. J Mech Phys Solids 48:1565–1595
72. Aifantis EC (1984) On the microstructural origin of certain inelastic models. Trans ASME J Eng Mater Technol 106:326–330
73. Mühlhaus H-B, Aifantis EC (1991) A variational principle for gradient plasticity. Int J Solids Struct 28:845–857
74. Zbib HM, Aifantis EC (1992) On the gradient-dependent theory of plasticity and shear banding. Acta Mech 92:209–225
75. de Borst R, Sluys LJ, Mühlhaus HB, Pamin J (1993) Fundamental issues in finite element analysis of localization of deformation. Eng Comput 10:99–121
76. Fleck NA, Hutchinson JW (2001) A reformulation of strain gradient plasticity. J Mech Phys Solids 49:2245–2271
77. Gurtin ME, Anand L (2009) Thermodynamics applied to gradient theories involving the accumulated plastic strain: the theories of Aifantis and Fleck and Hutchinson and their generalization. J Mech Phys Solids 57:405–421
78. Fleck NA, Hutchinson JW, Willis JR (2015) Guidelines for con- structing strain gradient plasticity theories. J Appl Mech 82:071002
79. Fleck NA, Hutchinson JW (1997) Strain gradient plasticity. In: Hutchinson JW, Wu TY (eds) Adv Appl Mech, vol 33. Academic Press, New York, pp 295–361
80. Gudmundson P (2004) A unified treatment of strain gradient plasticity. J Mech Phys Solids 52:1379–1406
81. Gurtin ME, Anand L (2005) A theory of strain-gradient plasticity for isotropic, plastically irrotational materials. Part I: small deformations. J Mech Phys Solids 53:1624–1649
82. Kuroda M (2015) A higher-order strain gradient plasticity theory with a corner-like effect. Int J Solids Struct 58:62–72
83. Kuroda M (2016) A strain-gradient plasticity theory with a corner-like effect: a thermodynamics-based extension. Int J Fract 200:115–125
84. Kuroda M (2015) Strain gradient plasticity: A variety of treatments and related fundamental issues. Adv Struct Mater 64:199–218
85. Kuroda M, Tvergaard V (2010) An alternative treatment of phenomenological higher-order strain-gradient plasticity theory. Int J Plast 26:507–515
86. Wang YW, Majlessi SA, Ning J, Aifantis EC (1996) The Strain Gradient Approach for Deformation Localization and Forming Limit Diagrams. J Mech Behavior Mater 7:265–277
87. Safikhani AR, Hashemi R, Assempour A (2008) The strain gradient approach for determination of forming limit stress and strain diagrams. Proc Inst Mech Eng, Part B: J Eng Manuf 222:467–483
88. Gurtin ME (2002) A gradient theory of single-crystal viscoplasticity that accounts for geometrically necessary dislocations. J Mech Phys Solids 50:5–32
89. Gurtin ME (2008) A finite-deformation, gradient theory of single-crystal plasticity with free energy dependent on densities of geometrically necessary dislocations. Int J Plast 24:702–725
90. Groma I, Csikor FF, Zaiser M (2003) Spatial correlations and higher-order gradient terms in a continuum description of dislocation dynamics. Acta Mater 51:1271–1281

91. Yefimov S, Groma I, van der Giessen E (2004) A comparison of a statistical-mechanics based plasticity model with discrete dislocation plasticity calculations. J Mech Phys Solids 52:279–300
92. Evers LP, Brekelmans WAM, Geers MGD (2004) Non-local crystal plasticity model with intrinsic SSD and GND effects. J Mech Phys Solids 52:2379–2401
93. Bayley CJ, Brekelmans WAM, Geers MGD (2006) A comparison of dislocation induced back stress formulations in strain gradient crystal plasticity. Int J Solids Struct 43:7268–7286
94. Kuroda M, Tvergaard V (2006) Studies of scale dependent crystal viscoplasticity models. J Mech Phys Solids 54:1789–1810
95. Kuroda M, Tvergaard V (2008) On the formulations of higher-order strain gradient crystal plasticity models. J Mech Phys Solids 56:1591–1608
96. Kuroda M, Tvergaard V (2008) A finite deformation theory of higher-order gradient crystal plasticity. J Mech Phys Solids 56:2573–2584
97. Kuroda M (2011) On large-strain finite element solutions of higher-order gradient crystal plasticity. Int J Solids Struct 48:3382–3394
98. Ekh M, Bargmann S, Grymer M (2011) Influence of grain boundary conditions on modeling of size-dependence in polycrystals. Acta Mech 218:103–113
99. Kuroda M (2013) Higher-order gradient effects in micropillar compression. Acta Mater 61:2283–2297
100. Bayerschen E, Böhlke T (2016) Power-law defect energy in a single-crystal gradient plasticity framework: a computational study. Comput Mech 58:13–27
101. Kuroda M (2017) Interfacial microscopic boundary conditions associated with backstress-based higher-order gradient crystal plasticity theory. J Mech Mater Struct 12:193–218
102. Kuroda M, Needleman A (2019) Nonuniform and localized deformation in single crystals under dynamic tensile loading. J Mech Phys Solids 125:347–359
103. Borg U (2007) Strain gradient crystal plasticity effects on flow localization. Int J Plast 23:1400–1416